How to ensure reliable connectivity for aerial vehicles over cellular networks

Nguyen, Huan Cong; Amorim, Rafhael Medeiros de; Wigard, Jeroen; Kovács, Istvan; Bundgaard Sørensen, Troels; Mogensen, Preben Elgaard

Published in:
IEEE Access

DOI (link to publication from Publisher):
10.1109/ACCESS.2018.2808998

Publication date:
2018

Document Version
Publisher's PDF, also known as Version of record

IEEE Access
Multidisciplinary | Rapid Review | Open Access Journal

SPECIAL SECTION ON NETWORKS OF UNMANNED AERIAL VEHICLES: WIRELESS COMMUNICATIONS, APPLICATIONS, CONTROL AND MODELLING

Received January 1, 2018, accepted February 5, 2018, date of publication February 23, 2018, date of current version March 19, 2018.

Digital Object Identifier 10.1109/ACCESS.2018.2808998

INVITED PAPER

How to Ensure Reliable Connectivity for Aerial Vehicles Over Cellular Networks

HUAN CONG NGUYEN[1], (Member, IEEE), RAFHAEL AMORIM[2], JEROEN WIGARD[2], ISTVÁN Z. KOVÁCS[2], TROELS B. SØRENSEN[2], AND PREBEN E. MOGENSEN[1,2]

[1]Department of Electronic Systems, Aalborg University, 9220 Aalborg, Denmark
[2]Nokia Bell Labs, 9220 Aalborg, Denmark

Corresponding author: Jeroen Wigard (jeroen.wigard@nokia-bell-labs.com)

This research has received funding from the SESAR Joint Undertaking under the European Union's Horizon 2020 research and innovation programme, grant agreement No 763601. The research is conducted as part of the DroC2om project.

ABSTRACT Widely deployed cellular networks are an attractive solution to provide large scale radio connectivity to unmanned aerial vehicles. One main prerequisite is that co-existence and optimal performance for both aerial and terrestrial users can be provided. Today's cellular networks are, however, not designed for aerial coverage, and deployments are primarily optimized to provide good service for terrestrial users. These considerations, in combination with the strict regulatory requirements, lead to extensive research and standardization efforts to ensure that the current cellular networks can enable reliable operation of aerial vehicles in various deployment scenarios. In this paper, we investigate the performance of aerial radio connectivity in a typical rural area network deployment using extensive channel measurements and system simulations. First, we highlight that downlink and uplink radio interference play a key role, and yield relatively poor performance for the aerial traffic, when load is high in the network. Second, we analyze two potential terminal side interference mitigation solutions: interference cancellation and antenna beam selection. We show that each of these can improve the overall, aerial and terrestrial, system performance to a certain degree, with up to 30% throughput gain, and an increase in the reliability of the aerial radio connectivity to over 99%. Further, we introduce and evaluate a novel downlink inter-cell interference coordination mechanism applied to the aerial command and control traffic. Our proposed coordination mechanism is shown to provide the required aerial downlink performance at the cost of 10% capacity degradation in the serving and interfering cells.

INDEX TERMS 3D coverage, aerial vehicles, cellular network, drone, LTE, interference management, reliable communication, propagation channel, UAV.

I. INTRODUCTION

The market for Unmanned Aerial Vehicles (UAVs), flying in the Very Low Level (VLL) airspace [1], is rapidly growing and emerging commercial use cases are being developed day by day. Besides aerial photography and film-making, UAVs become very useful for agricultural or pipe-line inspection, package delivery and disaster-relief applications. In general, it can be said that UAVs, also commonly referred to as *drones*, are used to streamline operations, to reduce risks and to improve efficiency [2].

Current regulations in most countries limit drone operations to the cases in which there is Visual Line of Sight (VLOS) between an UAV and its pilot. However, it is expected that Beyond Visual Line of Sight (BVLOS) operations will be allowed for extended flight range, provided there is a reliable Command and Control (C2) link to the drone. The C2 link is critical to safe operations of the drones. In the uplink (UL), i.e. from a drone to a Base Station (BS), the control link is used to update the Unmanned Aircraft System Traffic Management (UTM) or flight control unit with the drone location, plus potentially crucial information, such as telemetry and sensor readings, which the control function can utilize to make its decisions. In the downlink (DL), from BS towards the drone, the C2 link allows the control function to change the drone's flight path to avoid potential collisions, or to command a range of sensor/actuator functions on board of the drone. As one example, the DL C2 can be used to maneuver the UAV, when its originally-designed route crosses the path of a manned vehicle (e.g. helicopter) that suddenly needs to land for an emergency.

Cellular networks are an attractive solution to provide the C2 connectivity. In particular, current Long-Term Evolution (LTE) based systems present many advantages such as: an already in place infrastructure that provides almost full coverage, therefore minimizing the investments; shared resources with Terrestrial User Equipments (TUEs) to reduce the operational costs; flexible scheduler and multiple access to maximize resource usage efficiency. For very remote rural areas, and UAVs at the limit of VLL airspace, cellular coverage can be complemented with satellite. In this paper, we will concentrate on the parts of the network with full, or close to full, coverage. The biggest challenge is that cellular networks are not designed for aerial coverage, since their base stations typically use down-tilted antennas optimized for TUEs.

Not surprisingly various regulatory committees are striving for specifying the rules, which UAV operations must conform to, in order to ensure a robust and well-organized transition towards the ''Aerial Vehicles era''. It is critical that this transition shall occur without impacting the legacy functionalities and deployments. Among those organizations addressing UAV use cases, one can find also the Third Generation Partnership Project (3GPP), responsible for standardizing worldwide cellular technologies, such as Universal Mobile Telecommunications System (UMTS) (so-called: 3G) or LTE (4G). In March 2017, a 3GPP study item: ''Enhanced support for Aerial Vehicles'' was approved [3], aimed at preparing LTE networks to support a new type of User Equipment (UE), likely to emerge in cellular networks in the imminent future: airborne users flying at heights up to 300 m above the ground level. These works include the development of propagation channels and line-of-sight (LOS) probability models, and the assessment of coverage and capacity provided by cellular networks to UAV's connectivity [3].

It is important to note that several previous works have proposed the usage of UAVs as relay nodes and aerial BSs, for example [4], [5], in order to improve the overall system capacity, but this is a fundamentally different problem as the one we are trying to solve in this paper. Throughout this work, UAVs are treated as airborne UEs connected to terrestrial cellular networks.

The radio propagation channel for UAVs flying above buildings, terrain roughness and other forms of obstruction is considerably different from those observed by a TUE on the ground. For instance, the work in [6] shows that the LOS probability between a TUE and UAV increases monotonically with the elevation angle between the two devices, and therefore to UAV heights. Although this study is based on TUEs being served by a UAV-BS, the same rationale should apply to the case, where UAVs are users connected to the BS. Measurements conducted in [3] and [7] for the case of LTE showed the implications of higher UAV heights due to radio path clearance: higher number of neighbor cells observed, increased interference power, and reduced shadowing variation.

Besides radio clearance, the effect of antenna down-tilt should also be taken into account. As previously mentioned, the BS's antennas in cellular networks are down-tilted in order to optimize the terrestrial coverage, and this will impact the quality of the link between BS and UAV. The combination of the two effects are well described in [8], where the authors propose a channel model that adjusts a ground level model, by introducing a compensation function depending on the angle between UAV and BS. The reference for the model parameters are field measurements collected at 850 MHz for a BS with a monopole antenna. In [9], a modified two-ray model is presented to account for variations in the path loss exponent and antenna gains according to UE height.

FIGURE 1. Preparation for UAV channel measurement: Our pilot is mounting the R&S scanner on the DJI Matrice 600 drone.

In [10], a generic height-dependent channel model is proposed for UAV in a rural environment based on field measurements (see Figure 1), for heights up to 120m. Besides its simplicity, the model also provides a tool to evaluate the channel for different types of antennas, and captures the effects caused by side lobes of highly-directive antennas as commonly deployed in cellular systems. The simulations and analysis in this paper are performed using this channel model.

In cellular networks, the BS's inter-site distance (ISD) is designed according to ground level channel models and the density of TUEs. The ISD is therefore not optimized for the different propagation environment perceived by UAVs. As a result of this, and the radio path clearance, their radio performance tends to be negatively impacted due to a significant increase in interference levels [11]. Using the model in [10], the studies in [3] and [12] showed that highly loaded scenarios present a challenge for UAV coverage due to the interference levels observed, while the work presented in [13] disclosed that the interference mitigation gain depends significantly on the scenario's radio characteristics.

This paper presents an evaluation of specific UAV interference mitigation techniques by means of simulations, and its main goal is to evaluate how well existing techniques, traditionally optimized for TUEs, perform when applied to UEs mounted on drones. Different techniques are investigated for UL and DL cases, which are split in two groups: terminal-based and network-based solutions.

Terminal-based solutions assume UE operations are compatible with 3GPP's specifications, regarding power level and number of transmit antennas. The 3GPP Release 8 dictates that a UE can use 2, and up to 4 antenna elements [14]. Implementations with more elements is not practically precluded, provided the number of 'visible' elements to the radio network in any given transmission fulfill the 3GPP requirements. The size, geometry and degrees of freedom in the UAV movement, opens up several possibilities for multiple antenna deployments and interference mitigation techniques. As one example, the 3GPP study item [3] has concluded that the usage of beamforming solutions implemented on the UAV side presents the potential to increase the Signal to Interference plus Noise Ratio (SINR) in both DL and UL. Usually, UE-side beamforming imposes some additional challenges for deployments, such as high-complexity processing and proper handling of handover events. In this paper, a more simplistic approach is investigated, where UAV characteristics are explored to produce an array of directional antenna beams in combination with antenna selection on the UAV side.

Interference cancellation is another terminal-based solution investigated in this paper. 3GPP Release 8 UEs can implement either Interference Cancellation (IC) or Interference Rejection Combining (IRC), and the performance of these techniques in LTE networks have been previously evaluated for TUEs [15]. However, the interference observed by UAVs differ from previous models, as several interfering sources are expected instead of a few dominant ones [13]. In this paper we extend the evaluation of IC performance under such a new scenario.

The network-based solutions presented in this paper are restricted to practical interference mitigation schemes that do not require significant changes on the network side, i.e. without modifying the type or number of BS antenna elements, their tilts, or carrier frequencies (e.g. use of dedicated carriers). This ensures that that the LTE network remains optimized for TUEs. The first network-based solution considered in the paper is the optimization of UL Open Loop Power Control (OLPC) parameters. As UAVs tend to have lower propagation losses and higher number of interfering BSs compared to TUE, applying the same UL power constraints will result in UAVs radiating high interference power to many neighboring BSs. In this paper, we evaluate a solution where different power control settings are applied to UAVs and TUEs. The solution assumes that the network is capable of identifying the airborne state of UEs, which can be achieved for legacy networks [3], [16].

Different inter-cell interference coordination (ICIC) solutions have been previously studied for LTE, e.g. [17]. The general concept is that neighbor cells coordinate the data transmission to reduce the overall interference levels. In general, the improvements in SINR are obtained at the expense of capacity loss, as some BSs are prevented to transmit in some radio resources. Our paper proposes and evaluates the potential benefits and capacity costs of implementing a novel inter-cell coordination mechanism for the DL C2 traffic of the UAVs served in the network.

The remainder of this paper is organized as follows. Section II features an overview of the height-dependent channel model used. Section III describes our system level simulator and its key parameters, while reference simulation results are presented in Section IV. Assessments on the interference mitigation techniques are made in Section V and VI, and finally the conclusions are presented in Section VII.

II. HEIGHT-DEPENDENT RURAL PROPAGATION MODEL

In a previous study, we have performed a measurement campaign at two locations in Fyn, Denmark, to characterize the propagation channel between terrestrial BSs and UAVs in a rural scenario. The readers are encouraged to refer to [10] for detailed information on the measurement campaign, and the derivation of a large-scale path loss model for UAVs. Here the proposed height-dependent path loss model, which is applied in our simulations, is briefly presented for the sake of completeness. It takes the following form:

$$PL_{\text{AB}}(h_u, d) = 10\alpha_{h_u} \log_{10}(d) + \beta_{h_u} + X_{\sigma_{h_u}} \quad \text{[dB]} \quad (1)$$

where $PL_{\text{AB}}(h_u, d)$ is the mean path loss taking into account: (a) the 3-dimensional (3D) distance d between BS and UAV, and (b) the UAV's height h_u. Both distance and height are in meters. The term α_{h_u} is the path loss slope, β_{h_u} is the floating intercept (in dB), and $X_{\sigma_{h_u}}$ is a normal-distributed random variable with zero mean and standard deviation σ_{h_u}, which represents the large-scale shadow fading.

TABLE 1. Rural height-dependent UAV propagation model.

h_u	Model's Parameters			Detected Cells (average)
	α_{h_u}	β_{h_u}	σ_{h_u}	
Ground (1.5 m)	3.7	-1.3	7.6	5.1
15 m	2.9	7.4	6.2	6.1
30 m	2.5	20.4	5.2	7.6
60 m	2.1	32.8	4.4	11.6
120 m	2.0	35.3	3.4	16.9

The channel model parameters extracted from our measurements, according to the best-fit of 1, are presented in Table 1. It is important to note that they are changing with height: First, a slope of 3.7 at ground level is observed, which is close to that of existing rural propagation models, such as Okumura-Hata [18] or 3GPP non line-of-sight (NLOS) Rural Macro (RMa) [19] model. When the height of the UAV increases, the measured slope decreases and approaches the value of 2, i.e. free-space path loss. Second, the shadow fading variation, σ_{h_u}, is also reduced with height: Approximately 7.6 dB is observed at 1.5m, whereas at 120 m it is only 3.4 dB. Both indicate that the propagation path from a ground BS to an elevated drone is often clear from obstacles, which increases the received signal strengths seen at/from the drone. As a result, the number of neighboring cells detected by the drone is also increased with height, which implies stronger interference in both UL and DL [3], [12]. The interference

seen from the drone, or caused by it, will be analyzed in greater detail in Section IV. We assume that the propagation channel becomes height-independent after 120 m, since increasing height at this point does not improve the radio path clearance further. Therefore, the channel model's parameters at 120 m can be applied for higher heights.

III. SYSTEM LEVEL SIMULATOR

Our analysis is based on a simulation framework for quantitative investigation of user mobility, with focus on the 3GPP LTE technology, which is described in [20]–[22]. In this section we introduce the modeling assumptions, parameters and Key Performance Indicators (KPIs) used in our simulations.

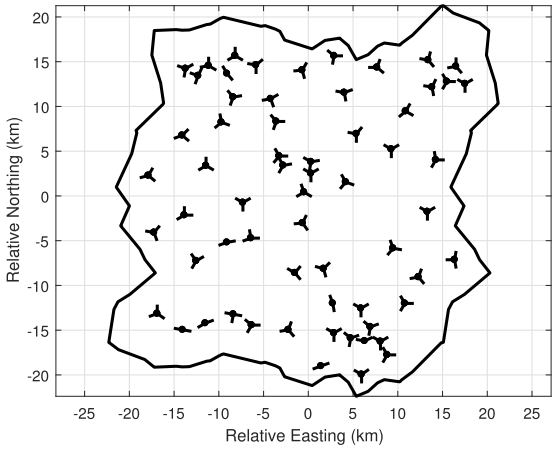

FIGURE 2. Rural network layout, including 179 cells, for simulation evaluation. Dark solid line demarcates network border.

A. MODELING ASSUMPTIONS

A network of C cells is considered, where each cell c is described by a set of properties, including its 3D position, antenna pattern, bearing, tilting and transmitting power. To make the study more realistic, an actual 800 MHz LTE network, depicted in Figure 2, is imported into our simulation: The network consists of 179 cells covering a 40 km × 40 km area in Fyn (Denmark), where the measurements presented in Section II have been performed. This is to ensure that the path loss model is applied in the same environment in which it was measured. The average ISD is 3 km, and the network is wrapped around to introduce interference at the network edge.

There are U users dropped uniformly in 2-dimension within the network. All TUEs are assumed to be at 1.5 m, while all UAVs are dropped at a given height, specified by the simulation scenario. The users move along linear trajectories in random directions through the network at a constant velocity. User mobility is constrained to be within the network border to remain in coverage. When a UE reaches the border, it will bounce back following a random direction. At time instant t the position of user u is described by the location function $p_u(t)$. We utilize the height-dependent propagation channel model, introduced in Section II, in the calculation of received power $R_c(p)$ from the antenna of cell c towards any location p on the map:

$$R_c(p) = P_{\mathrm{DL}} - PL_{\mathrm{AB}}(h_u, d_{c,p}) + G_c(\phi_{c,p}, \theta_{c,p}) \quad [\mathrm{dBm}] \tag{2}$$

where P_{DL}, measured in dBm, is the transmitting power from cell c, and G_c is the antenna gain (in dB) in the direction of location p. The $d_{c,p}$, $\phi_{c,p}$ and $\theta_{c,p}$ are the 3D distance, azimuth and elevation angle between cell c and location p, respectively. When UE is moving, all these parameters are time-dependent.

The cell c serving user u at time instant t is defined by the connection function $c = x_u(t) \in \{1, 2, 3...C\}$. As the user moves through the network, its serving cell can change via Handover (HO) procedure according to 3GPP specifications. The user continuously measures Reference Signal Received Quality (RSRQ) level from all cells, and once a neighboring cell becomes better than the serving cell by an offset Δ_{A3} for a period of time TTT, i.e. A3 event, the HO procedure is triggered. Using the approach in [20], the instantaneous wideband DL SINR $\gamma_{u,c}(t)$ of user u at time instant t (from the serving cell c) can be approximated by:

$$\gamma_{u,c}(t) = R_c(p_u(t)) - 10\log_{10}\left[\sum_{i\neq c}\rho_i(t)10^{\frac{R_i(p_u(t))}{10}} + 10^{\frac{N}{10}}\right] \quad [\mathrm{dB}] \tag{3}$$

in which N is the thermal noise power in dBm, and $\rho_i \in [0, 1]$ is the load in the i^{th} cell at time t, indicating that a cell with lower load, ρ_i is close to zero, produces lower interference.

The SINR determines how much DL throughput a user can get with a given number of assigned Physical Resource Blocks (PRBs). The UE is said to be in 'outage', if its DL SINR gets below a threshold Q_{out} such that communication is no longer possible. This might happen due to either too low signal from serving cell or too high total interference from all neighboring cells. Another threshold, Q_{in}, is defined as having much higher probability of reception than Q_{out}, and once the DL SINR is better than Q_{in} the communication channel is assumed to be back to normal. In our simulation, Q_{out} and Q_{in} are chosen according to [3] as −8 dB and −6 dB, respectively. The duration in which the user's SINR goes below threshold Q_{out} and until it becomes better than Q_{in} is defined as the *time in* Q_{out}. If the user is in Q_{out} for longer than a period of T_{310}, it is considered to experience a Radio Link Failure (RLF), and therefore a recovery procedure will be triggered, i.e. the user disconnects from the current cell and starts searching for a better serving cell.

In LTE, the UL power control is implemented as a combination of Open Loop Power Control (OLPC) and Closed Loop Power Control (CLPC) [23]. In this study, we focus only on the usage of OLPC, because it is simple and does not require feedback information from serving BS. The algorithm can be described as follows:

$$P_{\mathrm{UL}} = \min\left\{P_{\mathrm{UL}}^{\max}, \mathrm{P0} - \Delta_{\mathrm{P0}}^{u} + \alpha PL_{\mathrm{est}} + 10log_{10}M\right\} \quad [\mathrm{dBm}] \tag{4}$$

in which P_{UL} and $P_{\text{UL}}^{\max}$ are respectively the UE's actual and maximum allowed transmit power. P0 is a parameter designed according to the target Signal to Noise Ratio (SNR) [23]. Also, $\alpha \in [0, 1]$ is the fraction of estimated path loss (PL_{est}) to be compensated, and M represents the number of PRBs allocated to the UE in the UL. The term Δ_{P0}^{u}, called P0 offset, is specific to our approach for mitigating interference from UAVs, which is described in more details later in Section VI-A.

TABLE 2. Key simulation parameters.

Parameter	Value
Simulation area	40 x 40 km
Number of cells (C)	179 cells
Average network ISD	3.0 km
Cell's transmit power (P_{DL})	49 dBm
System bandwidth	20 MHz
Carrier frequency	800 MHz
MIMO configuration	2x2
2D shadowing correlation distance	100 m
Shadowing correlation	0.5 (sites), 1 (cells)
Total number of users (TUE + UAV)	1790 (average 10 per cell)
User velocity	30 km/h
TUE DL traffic	FTP model
TUE DL packet size	20 Mbit on average
UAV DL C2 traffic	CBR model
UAV DL C2 data rate	100 kbps
UL traffic for TUE and UAV	Full buffer model
Threshold Q_{out}	-8 dB
Threshold Q_{in}	-6 dB
RLF timer (T_{310})	1 s
RSRP and RSRQ measurement error	1.22 dB
HO event	A3 with $\Delta_{\text{A3}} = 2$ dB
HO Time to trigger (TTT)	160 ms
Maximum UL transmit power ($P_{\text{UL}}^{\max}$)	23 dBm
Power control P0	-98 dBm per PRB
Power control α	0.8

B. SIMULATION PARAMETERS AND KPIs

The most important parameters for our simulations are summarized in Table 2. The radio mobility parameters follow the assumptions used in the 3GPP Aerial Vehicle performance studies [3]. Each cell has 10 users on average, i.e. counting both TUEs and UAVs. In DL, the TUE traffic pattern is modeled as File Transfer Protocol (FTP) sessions, where both packet size and arrival time are Poisson-distributed random variables. By keeping the mean packet size constant at 20 Mbit and varying the mean arrival time from 20 to 80 s, we control the *downlink offered load* in the network. The load is measured as the percentage of PRBs being scheduled, averaged over all cells and simulation steps. The UAV is assumed to have only C2 data in DL, which is modeled as a Constant Bit Rate (CBR) traffic of 100 kbps, or equivalently 1250 Bytes every 100 ms. Our DL scheduler prioritizes the C2 traffic over the FTP traffic, meaning that the C2 will be scheduled first, and then the remaining resources will be divided equally among the connected TUEs which have FTP data to receive. Users are assumed to be in *idle-mode*, if there is no DL data to be transmitted. A user switches from idle to *connected-mode*, when DL packet arrives at the buffer, if it is not currently in RLF. Once the data buffer is clear, the user returns to idle-mode. For the UL data traffic of both TUEs and UAVs, we assume a full buffer traffic model, in which UL transmission is off when the DL is in either idle-mode or in RLF. In other words, the UL traffic load in our simulations will also be lower, when the DL offered load is reduced and/or when the outage probability is high due to RLF.

The main KPI's used in this paper for assessing the impact of deploying UAVs on the network performance are listed below. Each of these KPIs is evaluated separately for TUEs and UAVs.

- *DL SINR:* Average UE DL connected-mode SINR, which is the $\gamma_{u,c}(t)$ gathered under the condition that the UE has data to receive and not in RLF, and averaged over all UEs and time instants.
- *DL Throughput:* Average UE DL throughput, collected under the same condition as the DL SINR.
- *Outage Probability:* Estimated as percentage of time instants that a UE is in Q_{out} relative to the total simulation time, averaged over all UEs.
- *Average Time in Q_{out}* : Duration for time in Q_{out} averaged over all Q_{out} occasions and UEs.
- *UL SINR:* Average UE UL SINR, which is defined the same way as the DL SINR above, but for UL resources. Details on UL SINR calculation used in the simulations are found in [21].
- *UL Throughput:* Average UE UL throughput corresponding to the UL SINR.

IV. REFERENCE SIMULATION RESULTS

This section looks at the impact of UAV deployment on cellular network performance in both DL and UL. The performance numbers presented in this section are the reference points for discussing the gain of interference mitigation techniques in Sections V and VI.

A. DOWNLINK PERFORMANCE

Figure 3 shows the average SINR, which is collected for UAVs and TUEs separately, as a function of the offered load. The *Ref* refers to the case when all users in the network are TUEs, and the *Hxm* is where UAVs account for 1% users and fly at a constant height of x meters. As the traffic load increases, TUEs in the *Ref* case are subjected to only a slight DL SINR degradation: The average SINR drops from 3 dB to 1 dB as the offered load jumps from 10% to 67%. On the other hand, it is evident that the UAV SINR is a function of both network load and the height at which the UAVs are deployed. At the lowest load point, the UAVs experience better SINR than TUEs in general, partially due to the gain from better serving cell signal strength. However, when the load increases, their SINR drops quickly: At 120 m the UAV SINR falls from 7 dB to -5 dB, if network load increases from 10% to 67%. That is a significant 12 dB reduction, compared to merely 2 dB for TUEs in the same situation. It indicates that the UAV DL connection is much more sensitive to network

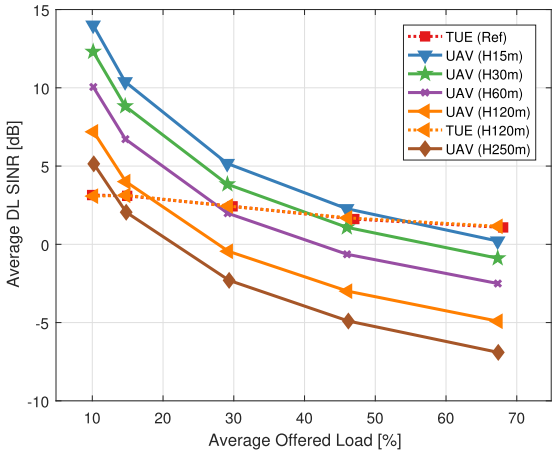

FIGURE 3. SINR experienced during data transmission vs. offered load. *Ref* indicates the case without any UAV, while *Hxm* refers to cases where UAVs accounts for 1% users in the network and fly at constant height of *x* m.

load than the TUE. The UAV SINR is also degraded with increasing height: At 67% load the SINR goes from 0 dB at 15 m to −7 dB at 250 m, corresponding to 7 dB degradation. This degradation is more or less constant vs. the offered traffic load points.

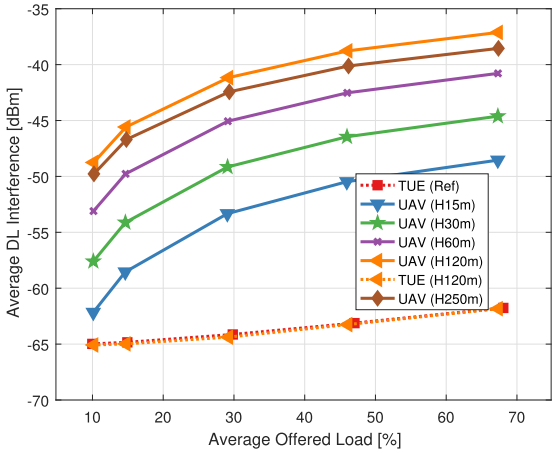

FIGURE 4. Interference experienced during data transmission vs. offered load. *Ref* indicates the case without any UAV, while *Hxm* refers to cases where UAVs accounts for 1% users in the network and fly at constant height of *x* m.

The DL SINR degradation can be explained by observing the average interference vs offered load introduced in Figure 4. Increasing the offered load leads to higher interference as expected, but the degradation is much faster for the UAVs than the TUEs: Up to 12 dB difference is experienced, when load changes from 10% to 67% for the UAVs at 120 m, while the corresponding value for the TUEs is only 3 dB. This is due to the fact that clearance of the radio propagation path for UAVs leads to improved signal strength from the serving cell, but also increased level of interference seen from the neighboring cells. The DL interference experienced by the UAVs is also a function of UAV height: It gradually increases until the UAVs reaches 120 m, and then decreases again. This is due to two reasons: Firstly, the path loss slope goes down steadily to 2, i.e. free-space path loss, for UAV heights from 15 m to 120 m, and remains constant with further increase of UAV height. Therefore, if the UAV is moving upwards up to 250 m, the path loss starts to increase because the 3D distance increases, while the slope is constant. Secondly, as the elevation angle increases with the UAV height, the BS antenna gain is also reduced, which might introduce further loss in the total link loss. The increase of total link loss reduces both serving cell's signal strength and neighboring cells interference, but nevertheless the combined effect is that the SINR is still reduced at 250 m compared to 120 m. From both Figure 3 and 4, we can see that the DL performance of the TUEs is not impacted by the presence of UAVs, since the TUE SINR and interference curves in *Ref* (no UAVs) and *H120m* case, i.e. 1% UAV flying at 120 m, are essentially identical.

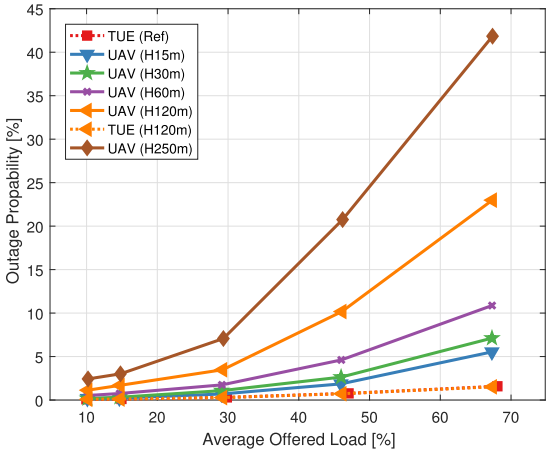

FIGURE 5. Outage probability vs. UAV height. *Ref* indicates the case without any UAV, while *Hxm* refers to cases where UAVs accounts for 1% users in the network and fly at constant height of *x* m.

Additionally, Figure 5 shows the outage probability as a function of offered load. Due to higher interference and thus worse DL SINR, the UAVs tend to suffer from larger outage than TUEs in general. At 67% load point, the outage probability for TUEs and UAVs at 120 m is 1.5% and 23%, respectively. Increasing the UAV height further to 250 m makes the situation even worse, i.e. the outage is increased to 42% for the same traffic load point. As the DL performance is essential for providing C2 link for drones, keeping outage probability low is critical. In the 3GPP discussions the target reliability was set to 99.9%, which could be understood that less than 0.1% outage is required. Similar to [3], our simulation results also indicate that downlink interference is a key obstacle to achieve the required DL performance, and therefore interference mitigation techniques are needed to improve the reliability of the C2 link in this type of deployment scenario.

To avoid swamping readers with results from all load points and heights, in the next sections we focus only on two

traffic load points, *medium* and *high*, which correspond to the 30% and 67% downlink load in Figures 3- 5, respectively. The UAV height is also often fixed at 120 m, unless otherwise stated.

B. UPLINK PERFORMANCE

This section discusses the impact of UAVs on the UL performance of the network.

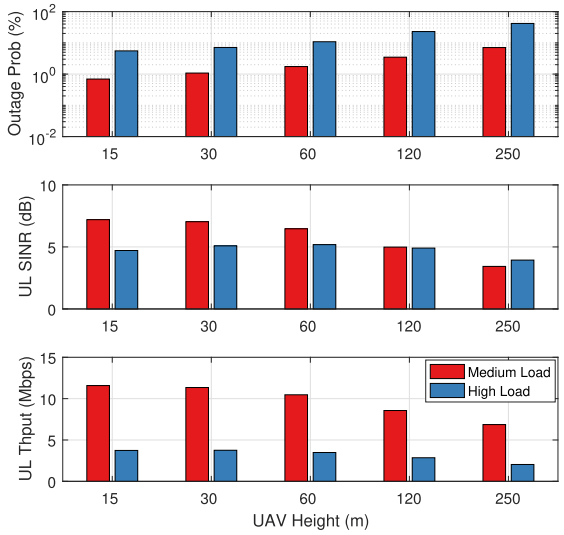

FIGURE 6. UAV outage probability, average UL SINR and throughput vs. UAV height. UAVs account for 1% users in the network and fly at a constant height.

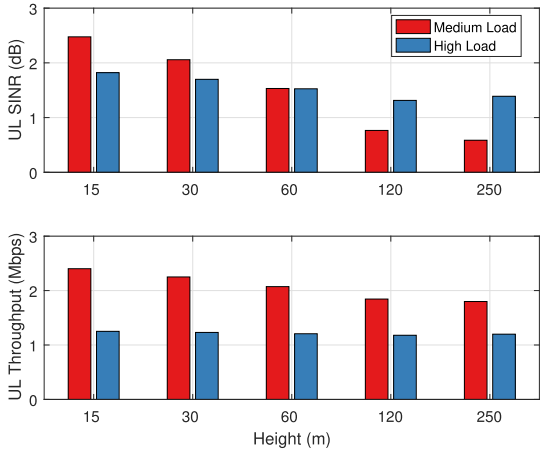

FIGURE 7. Average TUE UL SINR and throughput vs. UAV height. UAVs account for 1% users in the network and fly at a constant height.

Figure 6 illustrates the DL outage probability, average UL SINR and throughput for UAVs at different heights. Similarly, the UL performance of TUEs is shown in Figure 7. A few observations can be made: First, when an UAV flies at increased heights, it experiences better propagation conditions, and therefore its UL transmissions can potentially cause higher noise rise in the neighboring cells in a larger area compared to TUEs at the same location. Due to such an increase in UL interference, generally both UL SINR and throughput of UAVs and TUEs drop with increasing UAV height. This impact is less visible in the high load scenario, compared to the medium load one. At the high load, the UAV DL outage probability is much higher, i.e. many UAVs are in RLF and not able to transmit in UL, resulting in their lower impact in the network. Comparing the cases with UAVs at 15 m with 250 m in the medium load scenario, the UL SINR for TUEs reduces about 2 dB, while average UL throughput drops from 2.4 Mbps to 1.8 Mbps, or a 25% degradation. On the other hand, in the high load case, the UL SINR for TUEs is degraded by only 0.5 dB, and virtually no change in average UL throughput is visible. The higher UAV outage probability for UAV heights above 120 m also causes the TUE UL SINR in the high load scenario to be better than that of the medium load. Secondly, both UAV and TUE tend to achieve much higher UL throughput at medium load, because in this case, the available bandwidth is shared between a smaller number of active UEs. For example, an UAV at 120 m in the medium load scenario has in average three times more PRBs allocated than in the high load. Lastly, due to the improved propagation channel, UAVs always enjoy higher average connected-mode UL SINR and throughput than the TUEs.

In conclusion, the presence of UAVs has a negative impact on the UL performance of the TUEs. Again, interference mitigation techniques are likely to be required to reduce such impact, and in the next sections we will look at several candidate solutions for mitigating UAV interference and compare their performance.

V. TERMINAL-BASED INTERFERENCE MITIGATION TECHNIQUES

Assuming that no network upgrades are introduced, we consider first interference mitigation techniques applicable to the UE side. Techniques based on simple antenna combining and/or selection are achievable at a relatively low complexity, even when 3GPP Release 8 UEs are used on the UAVs. Here we select two potential schemes: antenna beam selection and interference cancellation.

A. ANTENNA BEAM SELECTION

Antenna selection with 2 or more directional antenna elements can be equivalent to a very simple beam selection, when assuming the antenna elements are mounted on the UAV body at the right spacing and angles/orientations. As an example, in case the UAV can rotate its fuselage in the azimuth plane while keeping the flight direction, then 1 or 2 antenna elements are sufficient to generate a 'beam' towards the serving cell. Or, in case the UAV degrees of freedom are more restricted, at least 4 antenna elements need to be mounted to provide four beams in the azimuth plane. In the elevation plane, the simple antenna selection described above might not be applicable, unless a larger number of antenna elements can be accommodated on the UAV fuselage. Certainly, higher gains can be expected when both azimuth and elevation antenna beamforming or selection is available.

Henceforth, our assumption is that antenna beam selection at the UAVs is applied only in the azimuth plane, and an omni-directional elevation radiation pattern is used.

We select an antenna beam radiation pattern modeled as a $sinc()^2$ function, with −3 dB beam-widths of approximately 90 deg, or 50 deg in the azimuth plane. The modeled beam patterns provide +6.6 dBi gain in the main direction and −13 dB front-to-sidelobe attenuation, which can be considered to account for the non-ideal orientation and/or shape of the beams. A simple setup with a grid of 2, 4 or 6 fixed beams is used (fixed relative to the UAV fuselage) to emulate a practical antenna selection mechanism. These options are depicted in Figure 8, along with the corresponding possible beam orientations on the UAV. Our choice for antenna beam model is different from the assumptions used in the 3GPP UAV studies reported in [3] and, in our opinion, provides a setup better aligned with all the other network and UAV deployment assumptions we make in this paper.

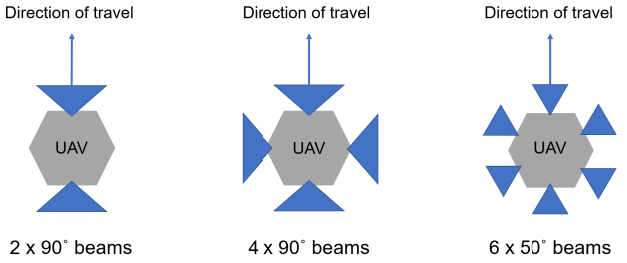

FIGURE 8. Modeled antenna beam configurations for the UAV.

The evaluated beam selection algorithm is based on the standard RSRQ measurements performed at the UAV terminal side, and without any requirement for feedback from the serving cell. First, for each detected cell, serving and interfering, the maximum RSRQ is determined across all the possible antenna beam orientations, i.e. 2, 4 or 6 beams, depending on the configuration used. This RSRQ, and the corresponding Reference Signal Received Power (RSRP) values, are used as input to the usual 3GPP mobility mechanisms, cell (re)selection and hand-over. In the second step, the antenna that maximizes the RSRQ for the serving cell is selected. We further assume that the same antenna beam orientation is used for both downlink and uplink transmissions, from and to the serving cell.

1) DOWNLINK RESULTS

Figure 9 shows the average downlink SINR and throughput improvements for the UAVs, when the antenna beam selection is applied (2, 4 or 6 fixed beams). The reference case, presented in Section IV, is assuming omni-directional UE antenna for UAVs, and is labeled as "0" number of beams.

In the medium load scenario, we can immediately notice a significant SINR improvement over the omni-directional case, already when using a grid of 2 fixed beams. In the high load case, the UAVs would need to use a grid of at least 6 fixed beams in order to experience similar SINR

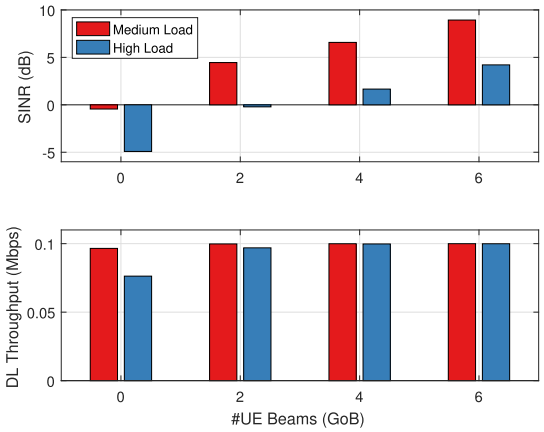

FIGURE 9. Average UAV DL SINR and throughput vs. number of antenna beams. UAVs account for 1% users in the network and fly at constant height of 120 m.

improvements. Analyzing the average throughputs, however, we can conclude that the target of 100 kbps is achievable in both low and high load conditions, when a grid of at least 4 fixed beams is used.

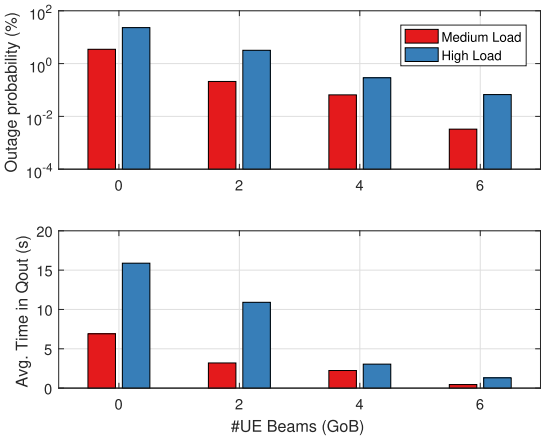

FIGURE 10. UAV outage probability and average time in Q_{out} vs. number of antenna beams. UAVs account for 1% users in the network and fly at constant height of 120 m.

Further, Figure 10 shows the outage probability and average time in Q_{out}, when antenna/beam selection is applied.

In the reference case, the outage probability is high, 5% and 22% for medium and high load cases, respectively. In order to achieve outage probabilities below 1%, similar to the conclusions from the downlink SINR analysis, the UAVs need to use a grid of at least 4 or 6 fixed beams, depending on the traffic load. It is remarkable that, when a grid of 6 beams is used, the outage can be as low as 0.1% even in the high traffic load case.

The average time in Q_{out} results show similar trends as the outage probability versus the number of beams used. Here the important conclusion is that only a minimum of 0.5 s and 1.2 s time in Q_{out} is achievable, even when a grid of 6 beams is used, improving significantly the interruption times that

should be taken into consideration in the design of the UAV communication link.

In order to disclose the impact of changing the number of UAVs, we have also analysed the cases when UAVs account for 10% users in the network. For brevity, these results are not shown here. The first conclusion is that the downlink performance of the UAVs depends on the number, and traffic demand, of the TUEs. This leads to results indicating performance improvement, especially in terms of outage and time in Q_{out}, when there are more UAVs and less TUEs in the network. The second conclusion is that the advantage from using antenna beams on the UAVs remains significant, and at 10% UAV penetration an outage probability below 0.01% can be achieved with a grid of 6 fixed beams.

Finally, it is confirmed that the downlink performance of the TUEs is not affected by the use of antenna beams at the UAVs, regardless of the UAV penetration. This is natural, due to the low UAV CBR traffic demand (100 kbps per UAV) relative to the high available cell capacity, and because the downlink transmissions to the UAVs generate the same amount of average inter-cell interference, with or without antenna beams at the UAVs. The TUEs can achieve average downlink throughputs of 6 Mbps and 2.5 Mbps in medium and high traffic load conditions, respectively. The average downlink performance of the TUEs is practically determined by the number of TUEs and their traffic demand.

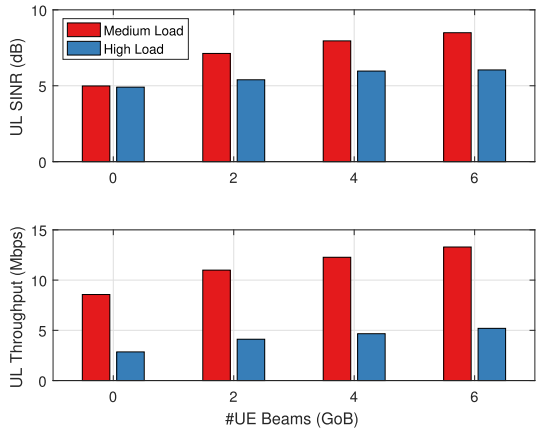

FIGURE 11. Average UAV UL SINR and throughput vs. number of antenna beams. UAVs account for 1% users in the network and fly at constant height of 120 m.

2) UPLINK RESULTS

Next we analyse the UL performance. Figure 11 shows the average UL SINR and throughput improvements for the UAVs, when the antenna beam selection is applied (2, 4 or 6 fixed beams). As a consequence of the favorable propagation conditions at 120 m height, the UAVs experience very good average UL SINR already without the use of antenna/beams. Nevertheless, the results show a non-negligible improvement in both average UL SINR and throughput, when a grid of 4 or 6 fixed beams is used, although more so in the medium load case.

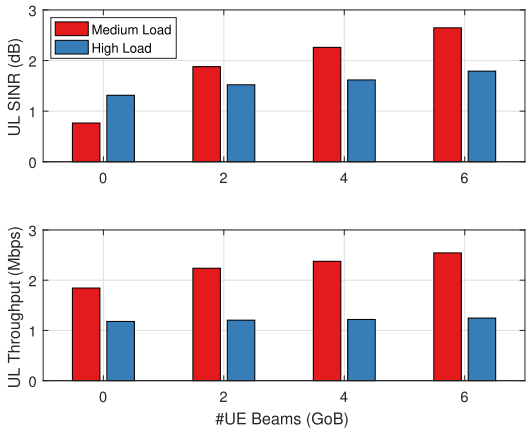

FIGURE 12. Average TUE UL SINR and throughput vs. number of antenna beams. UAVs account for 1% users in the network and fly at constant height of 120 m.

The impact of UAV antenna beam selection is visible on both the UL SINR and throughput for the TUEs in Figure 12. The use of a grid of 6 beams on the UAVs, results in up to 30% average throughput gain for the TUEs. This gain can be explained by the lower average inter-cell interference generated by the UAV UL transmissions due to their directional antenna beams.

The impact of the UAV penetration on the uplink performance KPIs for UAVs and for TUEs has been also investigated. For brevity, these results are not shown here. As expected, the increased number of UAVs leads to significantly lower UL performance for all UEs in the network: up to 36% and 45% degradation for UAVs and TUEs, respectively. The use of a grid of 6 beams on the UAVs remains beneficial, and can partially mitigate the increased interference, due to higher number of UAVs.

B. INTERFERENCE CANCELLATION

More recent LTE releases presented features to improve interference cancellation when compared to the baseline of a Release 8 UE. Release 11 was the first to introduce IRC, by adopting a Minimum Mean Square Error (MMSE) receiver, which suppresses interference by linearly combining the received signals at UE antennas [24]. In Release 12, non-linear processing is introduced with the Network-Assisted Interference Cancellation and Suppression (NAICS), which involves reconstructing the interfering signal and subtracting it before decoding the desired signal [24]. Even more advanced receivers are implemented in 3GPP Release 13 UE and beyond.

In this subsection, we quantify the potential of IC technique by assuming the perfect removal of 1 to 3 interferers. We note here that a 3GPP Release 13 UE with a minimum of 4 antenna elements would at best be able to cancel out 3 interfering signals; or alternatively, reject two strong interferers and receive data through the two remaining beams.

The ideal IC is modeled by canceling cells in order of the RSRP levels of the interfering cells, i.e. starting with the cell

with the strongest RSRP. A cell is included in the interference cancellation irrespective of its actual load. For the DL SINR this means that (3) is modified such that $\rho_i(t)$ equals zero for the i^{th} cell, whose signal is canceled out or ideally rejected by the UE receiver.

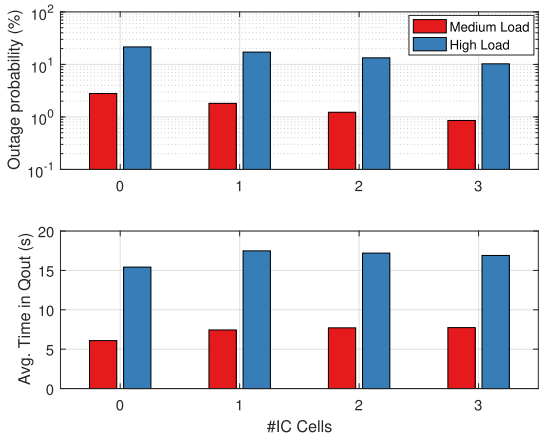

FIGURE 13. UAV outage probability and average time in Q_{out} vs. number of interfering cells whose signal was canceled. UAVs account for 1% users in the network and fly at constant height of 120 m.

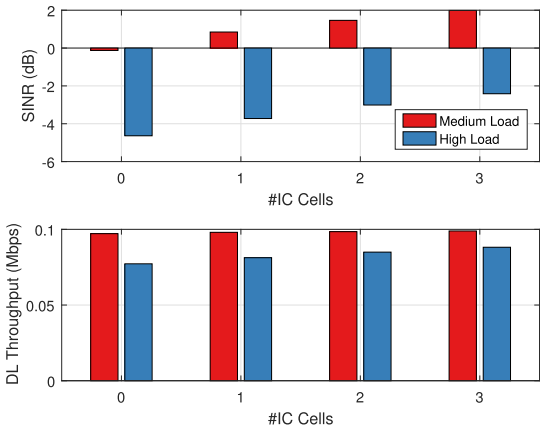

FIGURE 14. Average UAV DL SINR and throughput vs. number of interfering cells whose signal was canceled. UAVs account for 1% users in the network and fly at constant height of 120 m.

In Figure 13, we show the gain in terms of outage probability and average time in Q_{out} versus the number of cells canceled out for both the medium and high load cases. The outage decreases most for the high load case, as in the high load case removing the first x interfering cells reduces interference power more than in the case of low load. Also the time in Q_{out} decreases, but both the improvement in outage probability and average time in Q_{out} are in general lower than the improvements we have seen for the grid of fixed beams in the Section V-A. A reason for this is that part of the outage is caused by pure coverage issues, which cannot be improved by removing sources of interference. But it can be improved by a grid of fixed beams, which besides limiting the interference also provides a gain in the serving cell direction. This effect may also be observed in Fig. 14, where the high load case shows low SINR, and therefore, a high outage in throughput sense, even for 3 canceled interfering cells.

VI. NETWORK BASED INTERFERENCE MITIGATION SOLUTIONS

A. POWER CONTROL

In LTE networks, the power control parameters P0 and α, as in (4), are optimized in order to minimize the user's battery consumption and system's overall intra-cell interference, while maintaining good UL performance. In interference-limited networks, decreases in α, for example, will minimize the transmitted power of users close to cell edge. However, under-compensation of these parameters may cost significantly in terms of system throughput and UL outage. Usually, P0 and α are defined based on statistical information at BSs by network engineers.

Considering the significant differences in the propagation observed by TUEs and UAVs, we analyze the solution where the BSs use different settings for the different UE classes [3]. The term Δ^u_{P0} in (4) was introduced to introduce an offset in P0 for the different UE classes. In our study, it is zero for all TUEs, and a value between 0 and 12 dB for UAVs.

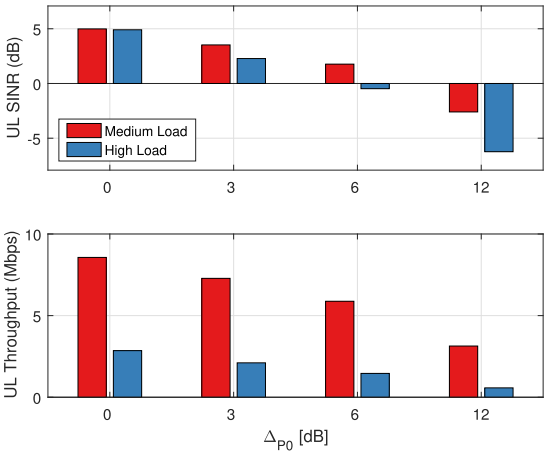

FIGURE 15. Average UAV UL SINR and throughput vs. UAV P0 offset. UAVs account for 1% users in the network and fly at constant height of 120 m.

Figure 15 illustrates the average UAV UL SINR and throughput, when Δ^u_{P0} increases from 0 to 12 dB for UAVs. As expected, when UAVs reduce their transmitted power, their SINR and throughput are also degraded. In the medium load scenario, the UAV throughput drops from 8.6 Mbps to 3.1 Mbps, or 64% reduction. This is the price to pay for using power control to reduce UAV's interference in the UL.

In Figure 16 the average TUE UL SINR and throughput are shown as function of UAV's P0 offset. When UAVs lower their transmitted power, interference is reduced, and therefore TUE's SINR and throughput are improved: Throughput increases from 1.8 Mbps to 2.8 Mbps, or 56%, when P0 goes from 0 to 12 dB in the medium load scenario, even though UAVs represent just 1% of the users. In the high load case,

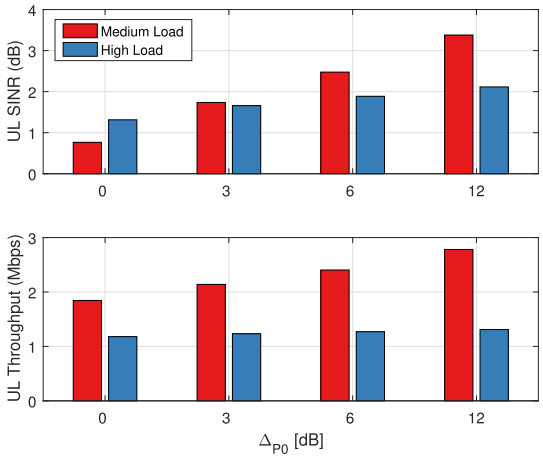

FIGURE 16. Average TUE UL SINR and throughput vs. UAV P0 offset. UAVs account for 1% users in the network and fly at constant height of 120 m.

due to a large number of UAVs are in outage, the effect of power control becomes much less significant. This approach has the advantage of not causing impact for TUEs output power distribution.

B. INTER-CELL INTERFERENCE COORDINATION

Several standardized inter-cell interference coordination solutions exist. The simplest downlink ICIC scheme was introduced in 3GPP Release 8, and is purely based on inter-cell signaling and does not require any UE-side functionality. The general idea is to coordinate the usage of radio resources between cells to optimize the cell edge SINRs. The enhanced and further enhanced ICIC (eICIC and feICIC) solutions have been developed in 3GPP Releases 10 and 11 for heterogeneous network deployments, targeting interference mitigation between macro base stations and small cells [17]. The main component is to suppress or blank sub-frames of the interfering BS. This allows the serving BS to schedule transmissions during these quiet sub-frames. When the Almost Blank Subframes (ABS) scheme is utilized, control channels can still be transmitted to ensure backwards compatibility. In LTE Release 11, the terminals are able to apply interference suppression as well, for better reception on the control signaling, allowing for "full blanking" of the downlink sub-frames.

The (f)eICIC solutions are applicable also between macro BSs, thus, in principle, can be considered as candidate solutions in our UAV investigations as well. The C2 link can be sent to an UAV according to the different generalized allocation schemes shown in Figure 17:

a) Dynamic scheduling (reference): scheduling the available data every Transmission Time Interval (TTI) according to proportional fair scheduling. This maximizes the scheduling gains, but is the most challenging scheme for the control signaling between cells, as very frequent coordination may be required, thus increasing the control plane load on X2.
b) Fixed PRB scheduling: scheduling every TTI, but on preallocated PRBs. This enables slow coordination between the cells, as the resources to be muted or transmitted at lower power in the interfering cells do not change frequently, but it comes at the cost of a lower frequency diversity gain.
c) Packing the data in few TTIs: in this scheme UAVs are only allowed to transmit every x^{th} TTI. The data for all served UAVs is packed in these TTIs, so that all neighboring cells easily can mute their resources in these TTIs. Coordination is rather simple, as the resources are well-known and semi-static. Benefit over the second scheme is that this scheme also provides interference coordination for the Physical Downlink Control Channel (PDCCH).

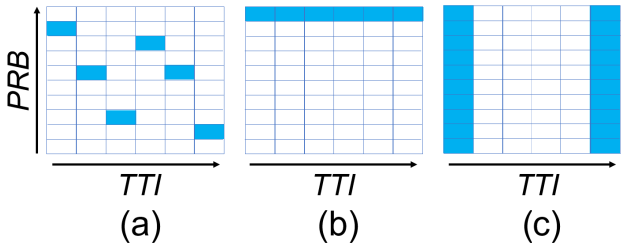

FIGURE 17. Different allocation schemes for the UAV C2 data: (a) dynamic scheduling, (b) fixed PRB scheduling, and (c) packing the data in a few TTIs.

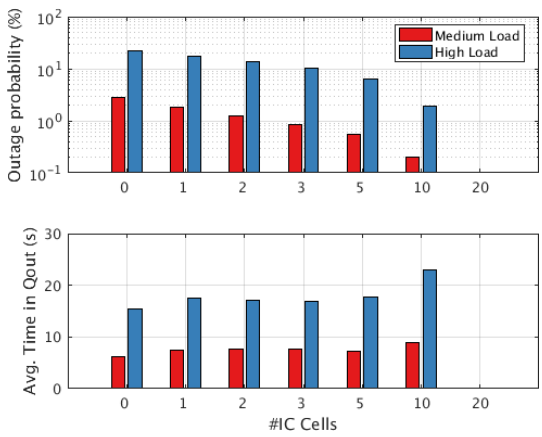

FIGURE 18. UAV outage probability, and average time in Q_{out} vs. number of IC cells muted. UAVs account for 1% users in the network and fly at constant height of 120 m.

We model the effect of blank sub-frames by assuming that the downlink transmission from the corresponding cells is muted in the corresponding TTIs and PRBs. For completeness we include here the cases where 1 up to 20 interfering cells are muted. We evaluate the impact of transmission muting in a similar way, as we did for the interference cancellation in Section V-B: (3) is modified so that $\rho_i(t)$ equals zero for the i^{th} cell, whose signal is muted. In Figure 18, we show the gain in terms of outage probability and average time in Q_{out} versus the number of cells muted for both the medium and high traffic load cases. The results for up to 3 cells muted are the same as presented in Section V-B. The notable result

TABLE 3. Considered scheduling configurations for downlink UAV C2 traffic.

#UAV	TTI	#PRB	Required SINR
1	Every	9	-6.0 dB
1	10^{th}	80	-4.7 dB
1	50^{th}	100	1.6 dB
2	Every	9	-6.0 dB
2	10^{th}	80	-4.0 dB
2	50^{th}	100	-6.0 dB
4	Every	9	-6.0 dB
4	10^{th}	80	-2.3 dB
4	50^{th}	100	14.6 dB

is the extreme case when the strongest 20 interfering cells are muted and the resulting outage drops below 0.01%. This indicates that the scenario becomes practically noise limited from the UE perspective, even in the high load scenario.

In the following, we compare the scheduling configurations shown in Table 3. In the first column, the number of UAVs in the serving cell are listed, the second column shows how often in time domain the UAVs are scheduled, the third and fourth column list the required number of PRBs and required SINR for the most conservative Modulation and Coding Scheme (MCS) possible to deliver C2 link data to an UAV. Note that we only consider UAVs in the serving cell, and assume for now that there are no UAVs in the cells around the serving cell. All UAVs are always scheduled in the same TTI, to minimize potential coordination signaling between cells. The required DL SINR is the maximum between the minimum required SINR for the PDCCH (-6 dB at 2% error rate [25]) and the required SINR for reaching 10% Block Error Rate (BLER) at the first transmission. We consider that every UAV sends 1250 B every 100 ms and one full retransmission is considered to reach high reliability.

It can be seen from the Table 3 that when we pack the UAV's transmission in fewer TTIs, or when we pack more UAVs in a TTI, the required SINR increases as the MCS increases, due to the data to be sent in less PRBs. Now the question is, how we can achieve the required SINR for the different cases, and how many cells we need to mute. This can be deducted from the curves shown in Figure 19, where the cumulative distribution function (CDF) of the DL SINR in high load is shown for a different number of interfering cells muted. We can see that if the required SINR is -6 dB, then we need to remove 3 cells in the case of high traffic load, to obtain an outage below 10%.

By comparing the CDFs from Figure 19 and the required SINR from Table 3 we can find the number of cells to be muted for the different cases. The result of this comparison is summarized in Table 4, where also the medium load case is represented.

It can be seen that at medium load, as long as we do not pack the UAVs data in very few TTIs, no coordination is needed, while at high load, medium to extensive coordination is needed. Note that scheduling every TTI becomes PDCCH limited at high load, which means we need to mute full

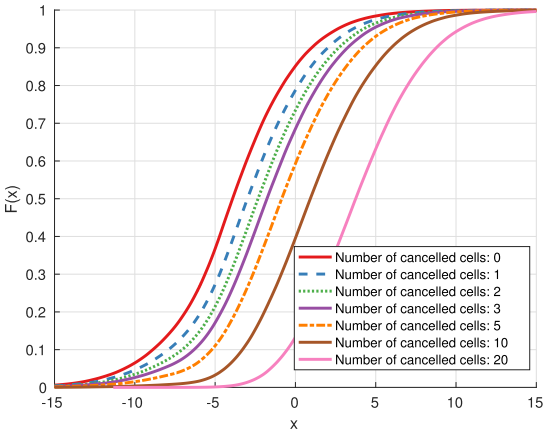

FIGURE 19. UAV DL SINR distribution in high load scenario. UAVs account for 1% users in the network and fly at constant height of 120 m.

TABLE 4. Number of cells to be muted in case of low load and high load for the considered scenarios.

#UAV	TTI	Muted Cell(s)		Capacity Loss	
		Medium	High	Medium	High
1	Every	0	3	9%	309%
1	10^{th}	0	8	8%	90%
1	50^{th}	10	20	20%	40%
2	Every	0	3	18%	318%
2	10^{th}	0	9	10%	110%
2	50^{th}	>20	$\gg$20	>40%	N/A
4	Every	0	3	36%	336%
4	10^{th}	0	14	10%	110%
4	50^{th}	>20	$\gg$20	>40%	N/A

TTIs. Therefore, scheduling every 10^{th} TTI becomes the most attractive option, as it does not require coordination between more than 10 cells. The last two columns of Table 4 show the loss in available capacity for TUEs as percentage of full cell capacity. It can be seen that the coordination is costly, especially in the high load case. With one UAV in the cell and scheduling it every 10^{th} TTI, it corresponds to losing 90% of a full cell capacity (shared over 9 cells). With one UAV, it is more attractive to schedule it every 50^{th} TTI, leading to a loss of 40% but spread over 20 cells. When having more UAVs, the scheduling needs to be more often and the capacity loss increases. Note that having 2 UAVs, which requires muting over 9 cells, corresponds to 2 drones per 10 cells, twice as much as the low drone density in the simulations shown in the previous sections.

Even though coordination may only be required between 10 cells, it may require coordination over a large area, as is shown in Figure 20, where the CDF of the distance to the x^{th} interfering cell can be seen. It can be seen that the strongest interferer may be as far away as 15 km, while capturing the first 10 cells with 90% likelihood requires covering an area of 20 km around the serving cell. However, the coordination for the C2 link can be rather slow, as the traffic can be assumed to be rather constant and therefore the TTI's to be coordinated do not change often. If there are also UAVs in

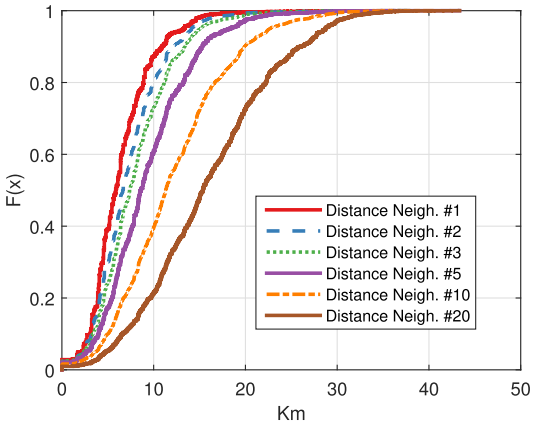

FIGURE 20. CDF of the distance to the strongest interferers for the rural area in Denmark.

the neighboring cells, they can be coordinated by fixing the PRB per UAV, i.e. allocating frequency slices to each of them in a rather static fashion.

VII. CONCLUSION

Widely deployed cellular networks are an attractive solution to provide large scale radio connectivity to aerial vehicles. One main prerequisite is that co-existence and optimal performance for both aerial and terrestrial users should be provided even though deployments are primarily optimized to provide good service for terrestrial users. In this paper, we investigate the performance of aerial radio connectivity in a typical rural area network deployments, using extensive channel measurements and system simulations. We highlight that downlink and uplink radio interference play a key role and yield relatively poor performance for the aerial traffic when load is high in the network. As a consequence, we analyze two groups of interference mitigation schemes under the constraint of minimal network upgrades required: terminal based and network based solutions.

In terms of terminal based interference mitigation solutions, we show that interference canceling and antenna beam selection can both improve the overall, aerial and terrestrial, system performance to a certain degree, with up to 30% throughput gain and an increase in the reliability of the aerial radio connectivity to above 99%. As network based solutions, we have analyzed the open loop uplink power control and a novel downlink inter-cell interference coordination. By setting a 3 dB to 6 dB lower P0 value for aerial users compared to the terrestrial users, the uplink power control mechanism can improve the average uplink throughput performance of terrestrial users. This improvement comes, however, at the cost of a degraded uplink throughput for aerial aerial users, and indicates that the power control alone might not be sufficient to adequately mitigate uplink interference.

Our proposed downlink inter-cell interference coordination mechanism is applied to the aerial users' command and control traffic. We show that inter-cell coordination is required in high load scenario, and up to 8 cells need to be muted to support 1% aerial user penetration. The cost of this solution is 10% terrestrial capacity degradation in each of the muted cells.

The results summarized above indicate that some practical, and relatively low complexity, interference mitigation schemes have good potential, when utilized in currently deployed rural LTE networks. Our findings also highlight that there are clear limitations of these interference mitigation techniques, especially when the overall network performance needs to be maintained for higher penetration of connected aerial vehicles. It is therefore also clear that further research and standardization activities are needed.

ACKNOWLEDGMENT

We would like to thank Steffen Hansen, our drone pilot, and other colleagues at Aalborg University for supporting this work. The research is conducted as part of the DroC2om project.

REFERENCES

[1] (Feb. 2017). *RPAS Air Traffic Management (ATM) Concept of Operations (CONOPS), European Organisation for the Safety of Air Navigation (EUROCONTROL)*. [Online]. Available: http://www.eurocontrol.int/publications/

[2] Business Insider Intelligent Report. (Jun. 2016). *Drones are About to Fill the Skies Within the Next 5 Years*. [Online]. Available: http://www.businessinsider.com/

[3] *Study on Enhanced LTE Support for Aerial Vehicles (Release 15)*, document 3GPP TR 36.777 V0.4.0 (2017-11), 3GPP, Technical Specification Group Radio Access Network, 2017.

[4] M. Mozaffari, W. Saad, M. Bennis, and M. Debbah, "Unmanned aerial vehicle with underlaid device-to-device communications: Performance and tradeoffs," *IEEE Trans. Wireless Commun.*, vol. 15, no. 6, pp. 3949–3963, Jun. 2016.

[5] Z. Xiao, P. Xia, and X.-G. Xia, "Enabling UAV cellular with millimeter-wave communication: Potentials and approaches," *IEEE Commun. Mag.*, vol. 54, no. 5, pp. 66–73, May 2016.

[6] A. Al-Hourani, S. Kandeepan, and S. Lardner, "Optimal LAP altitude for maximum coverage," *IEEE Wireless Commun. Lett.*, vol. 3, no. 6, pp. 569–572, Dec. 2014.

[7] B. Van Der Bergh, A. Chiumento, and S. Pollin, "LTE in the sky: Trading off propagation benefits with interference costs for aerial nodes," *IEEE Commun. Mag.*, vol. 54, no. 5, pp. 44–50, May 2016.

[8] A. Al-Hourani and K. Gomez, "Modeling cellular-to-UAV path-loss for suburban environments," *IEEE Wireless Commun. Lett.*, vol. 7, no. 1, pp. 82–85, Feb. 2018.

[9] N. Goddemeier, K. Daniel, and C. Wietfeld, "Role-based connectivity management with realistic air-to-ground channels for cooperative UAVs," *IEEE J. Sel. Areas Commun.*, vol. 30, no. 5, pp. 951–963, Jun. 2012.

[10] R. Amorim, H. Nguyen, P. Mogensen, I. Z. Kovács, J. Wigard, and T. B. Sørensen, "Radio channel modeling for UAV communication over cellular networks," *IEEE Wireless Commun. Lett.*, vol. 6, no. 4, pp. 514–517, Aug. 2017.

[11] M. M. Azari, F. Rosas, A. Chiumento, and S. Pollin, "Coexistence of terrestrial and aerial users in cellular networks," in *Proc. IEEE Globecom*, Singapore, Dec. 2017, pp. 1–6.

[12] H. C. Nguyen, R. Amorim, J. Wigard, I. Kovács, and P. Mogensen, "Using LTE networks for UAV command and control link: A rural-area coverage analysis," in *Proc. IEEE Veh. Technol. Soc.*, Sep. 2017, pp. 1–6.

[13] I. Z. Kovács, R. de Amorim, H. C. Nguyen, J. Wigard, and P. E. Mogensen, "Interference analysis for UAV connectivity over LTE using aerial radio measurements," in *Proc. IEEE 86th Veh. Technol. Conf. (VTC Fall)*, Toronto, ON, Canada, Sep. 2017, pp. 1–5.

[14] M. Kottkamp, A. Roessler, and J. Schlienz, "LTE-advanced technology introduction," Rohde & Schwarz, Munich, Germany, White Paper 08.2012-1MA169_3E, Aug. 2012.

[15] Y. Ohwatari, N. Miki, T. Asai, T. Abe, and H. Taoka, "Performance of advanced receiver employing interference rejection combining to suppress inter-cell interference in LTE-advanced downlink," in *Proc. IEEE Veh. Technol. Conf. (VTC Fall)*, San Francisco, CA, USA, Sep. 2011, pp. 1–7.
[16] J. Wigard, R. Amorim, H. C. Nguyen, I. Kovács, and P. Mogensen, "Method for detection of airborne UEs based on LTE radio measurements," in *Proc. IEEE 28th Annu. Int. Symp. Pers., Indoor, Mobile Radio Commun.*, Oct. 2017, pp. 1–6.
[17] K. I. Pedersen, B. Soret, S. B. Sanchez, G. Pocovi, and H. Wang, "Dynamic enhanced intercell interference coordination for realistic networks," *IEEE Trans. Veh. Technol.*, vol. 65, no. 7, pp. 5551–5562, Jul. 2016.
[18] M. Hata, "Empirical formula for propagation loss in land mobile radio services," *IEEE Trans. Veh. Technol.*, vol. VT-29, no. 3, pp. 317–325, Aug. 1980.
[19] *Study on Channel Model for Frequencies From 0.5 to 100 GHz*, document TR 38.901, 3GPP, Technical Specification Group Radio Access Network, Mar. 2017.
[20] I. Viering, M. Dottling, and A. Lobinger, "A mathematical perspective of self-optimizing wireless networks," in *Proc. IEEE Int. Conf. Commun.*, Dresden, Germany, Jun. 2009, pp. 1–6.
[21] I. Viering, A. Lobinger, and S. Stefanski, "Efficient uplink modeling for dynamic system-level simulations of cellular and mobile networks," *EURASIP J. Wireless Commun. Netw.*, vol. 2010, p. 282465, Aug. 2010.
[22] I. Viering, B. Wegmann, A. Lobinger, A. Awada, and H. Martikainen, "Mobility robustness optimization beyond Doppler effect and WSS assumption," in *Proc. 8th Int. Symp. Wireless Commun. Syst.*, Aachen, Germany, Nov. 2011, pp. 186–191.
[23] R. Mullner, C. F. Ball, K. Ivanov, J. Lienhart, and P. Hric, "Contrasting open-loop and closed-loop power control performance in UTRAN LTE uplink by UE trace analysis," in *Proc. IEEE Int. Conf. Commun.*, Dresden, Germany, Jun. 2009, pp. 1–6.
[24] H. Holma, A. Toskala, and J. Reunanen, *LTE Small Cell Optimization: 3GPP Evolution to Release 13*. Hoboken, NJ, USA: Wiley, 2016.
[25] D. Laselva, F. Capozzi, F. Frederiksen, K. I. Pedersen, J. Wigard, and I. Z. Kovács, "On the impact of realistic control channel constraints on QoS provisioning in UTRAN LTE," in *Proc. IEEE VTC Fall*, Sep. 2009, pp. 1–5.

HUAN CONG NGUYEN received the B.Sc. degree from the Hanoi University of Technology, Vietnam, in 1997, and the M.Sc. and Ph.D. degrees in electronics engineering from Aalborg University, Denmark, in 2004 and 2008, respectively. He is currently an Associate Professor with the Wireless Communication Networks Section, Department of Electronic Systems, Aalborg University, and External Researcher with Nokia Bell Labs, Aalborg, Denmark. He has over 50 journal and conference papers, in which he has authored or co-authored. He has over 10 year experience in the field of wireless communications, where his research interest includes synchronization, interference cancellation, cognitive radio, spectrum sharing, propagation channel modeling, and heterogeneous network evolution. He is currently with cellular-based connectivity for drones under the European DroC2om Project.

RAFHAEL AMORIM received the B.Sc. and M.Sc. degrees in electrical engineering from the Universidade de Brasília, Brazil, in 2009 and 2011, respectively. He is currently pursuing the Ph.D. degree in wireless communications, Aalborg University, Denmark. His research interests are related to radio propagation, PHY layer development and optimization and, more recently, in the connectivity of UAVs over cellular networks.

JEROEN WIGARD received the M.Sc. degree electrical engineering from Technische Universiteit Delft, Netherlands, in 1995 and the Ph.D. degree on the topic of handover algorithms and frequency planning in frequency hopping GSM networks from Aalborg University, Denmark, in 1999. He joined Nokia Aalborg, Denmark, where he was on radio resource management related topics for 2G, 3G, 4G, and 5G. He also has been studying several network deployment aspects related to LTE network evolution. He is currently with the Nokia Denmark Bell Labs, Aalborg (former Nokia Networks Aalborg) and involved in several IoT related topics, including drones and related connectivity issues. He has authored and co-authored over 40 journal and conference papers.

ISTVÁN Z. KOVÁCS received the B.Sc. degree from the Politehnica Technical University of Timisoara, Romania, in 1989, the M.Sc. degree in electrical engineering from École Nationale Supérieure des Télécommunications de Bretagne, France, in 1996, and the Ph.D. electrical engineering in wireless communications from Aalborg University, Denmark, in 2002. He currently has the position of senior wireless networks specialist with Nokia, Aalborg, Denmark, where he conducts research on radio connectivity evolution for machine type and aerial vehicle communications in LTE and 5G networks.

TROELS B. SØRENSEN received the M.Sc. degree in electrical engineering and the Ph.D. degree in wireless communications from Aalborg University in 1990 and 2002, respectively. He was with a Danish Telecom Operator developing type approval test methods. Since 1997, he has been with Aalborg University, where he is currently an Associate Professor with the Wireless Communication Networks Section, Department of Electronic Systems. His current research and teaching activities include cellular network performance and evolution, radio resource management, and related experimental activities.

PREBEN E. MOGENSEN received the M.Sc. and Ph.D. degrees from Aalborg University in 1988 and 1996, respectively. Since 2000, he has been a Full Professor and leading the Wireless Communication Networks Section, Department of Electronic Systems, Aalborg University. He has supervised over 35 successfully finalized Ph.D. candidates and has co-authored over 300 papers in various domains of wireless communication. Since 1995, he has also been part time associated with Nokia, and currently in a position of principal engineer with Nokia Bell Labs. His current research focus is on 5G and MTC/IoT.